

1 **The Apparent Absence of Kilometer-sized Pyroclastic Volcanoes on Mercury: Are We** 2 **Looking Right?**

3 **P. Brož^{1*}, O. Čadek², J. Wright³, and D. A. Rothery³**

4 ^{1*}Institute of Geophysics of the Czech Academy of Science, Boční II/1401, 141 31, Prague, Czech
5 Republic.

6 ²Charles University, Faculty of Mathematics and Physics, Department of Geophysics, V
7 Holešovičkách 2, 180 00, Prague, Czech Republic.

8 ³School of Physical Sciences, Open University, Milton Keynes MK7 6AA, United Kingdom.

9 Corresponding author: Petr Brož (petr.broz@ig.cas.cz)

10 **Key Points:**

- 11 • Kilometer-sized constructional explosive volcanoes have not been identified on Mercury
12 despite high-resolution data.
- 13 • Instead of steep constructional volcanoes, as on Earth and Mars, Mercurian pyroclastic
14 deposits likely form a wide and gentle blanket.
- 15 • Pyroclastic cones may not form at all on airless bodies; such landforms already recognized
16 on the Moon and Io are likely composite cones.
17

18 **Plain Language Summary**

19 Volcanic eruptions have occurred on planetary bodies throughout the Solar System,
20 including Mercury. Eruptions have different styles, which affect the volcanoes they build. On
21 Earth, small-volume explosive eruptions, which occur because expanding gas bubbles in the
22 magma fragment the erupting molten rock, can form piles of material called scoria cones. Features
23 resembling scoria cones have been observed on the Moon and Mars, but not yet on Mercury. We
24 used computer simulations to calculate where rock chunks would accumulate during explosive
25 eruptions with different eruption volumes, speeds, and angles, under Mercury gravity. We found
26 that, under most plausible scenarios, explosive eruptions on Mercury ejected material over too
27 great an area to build a cone, but instead built gentle slopes that would be undetectable in data
28 from the MESSENGER mission. This is because Mercury has no atmosphere to reduce the
29 maximum range of ejected rock and cause it to build up close to the vent. We suggest that
30 BepiColombo, the next spacecraft to visit Mercury, should concentrate on searching for
31 compositional, rather than topographical, evidence for explosive volcanism. We suggest that
32 volcanic cones on the Moon may have formed differently to scoria cones on Earth, since the Moon
33 also has no atmosphere.

34 **Abstract**

35 Spacecraft data reveal that volcanism was active on Mercury. Evidence of large-volume
36 effusive and smaller-scale explosive eruptions has been detected. However, only large (>~15 km)
37 volcanic features or vents have been found so far, despite abundant high-resolution imagery. On
38 other volcanic planets, the size of volcanoes is anti-correlated with their frequency; small
39 volcanoes are much more numerous than large ones. Here, we present results of a numerical model

40 that predicts the shapes of ballistically emplaced volcanic edifices and hence can explain the lack
41 of kilometer-sized constructional explosive volcanoes on the surface of Mercury. We find that due
42 to the absence of the atmosphere, particles are spread on this planet over a larger area than is typical
43 for Earth or Mars. Erupted volumes are likely insufficient to build edifices with slope angles that
44 enable their easy recognition with currently available data or that could survive destruction by
45 subsequent impact bombardment.

46 **1 Introduction**

47 Images obtained from the MErcury Surface, Space ENvironment, GEochemistry, and
48 Ranging (MESSENGER) mission have revealed evidence of effusive (e.g., *Head et al.*, 2008;
49 2011; *Byrne et al.* 2016) and explosive (e.g., *Head et al.*, 2009; *Thomas et al.*, 2014a; 2014b;
50 *Jozwiak et al.*, 2018) volcanism on the surface of planet Mercury. While the products of putative
51 effusive volcanism are in the form of solidified lavas forming the majority of the planet's smooth
52 plains units, covering around 27% of the planet's surface (*Head et al.*, 2011; *Denevi et al.*, 2013),
53 the explosive products are characterized by bright spots (dozens of kilometers across, and recently
54 allocated the descriptor term *facula/faculae*) with diffuse boundaries and without substantial
55 positive topographic expression. These faculae often contain an irregular depression in their
56 centers (e.g., *Kerber et al.*, 2009; *Thomas et al.*, 2014a) and are overwhelmingly located near
57 impact craters and faults (*Klimczak et al.*, 2018). While explosive vents are of the scale of
58 kilometers to tens of kilometers, vents associated with effusive volcanism are almost wholly
59 absent, presumably because they are buried by large volumes of highly mobile lavas capable of
60 flowing over long distances. Interestingly no kilometer-sized volcanic constructional edifices have
61 been unambiguously recognized on Mercury to date despite considerable searching.

62 The only exceptions observed so far are two kilometer-sized landforms that may represent
63 individual volcanic cones: one situated within the Heaney impact crater and the other near the
64 northwest edge of the Caloris basin (*Wright et al.*, 2018). Each of these has a central summit crater,
65 and their shapes are consistent with their formation by effusion of relatively viscous lavas. Their
66 volcanic origin is also favored from their geological context; they are situated within the areas
67 where volcanism almost certainly occurred in the past. However, their origin by nonvolcanic
68 means cannot be excluded due to the limitations in the resolution of MESSENGER data (*Wright*
69 *et al.*, 2018). Nevertheless, regardless of the mechanism of their origin, the extreme scarcity of
70 kilometer-sized constructional volcanic edifices is a surprising fact itself, as such features are
71 frequent on other terrestrial bodies within the Solar System where volcanism has taken place, such
72 as Earth (*Kereszturi & Németh*, 2013), the Moon (e.g., *Lawrence et al.*, 2013) and Mars (e.g.
73 *Hauber et al.*, 2009; *Brož & Hauber*, 2012; *Brož et al.*, 2015, 2017). On those bodies, the observed
74 kilometer-sized volcanoes are results of the accumulation of low volumes of lava and/or
75 pyroclastic material in the immediate vicinity of the vents from which the material was erupted by
76 effusive or explosive means.

77 The scarcity of kilometer-sized volcanoes on Mercury led *Wright et al.* (2018) to propose
78 that volcanic eruptions with sufficiently low eruption volumes and rates and short flow lengths,
79 which would be suitable for the construction of low-volumetric volcanoes by effusive lavas, were
80 highly spatiotemporally restricted during the preserved portion of Mercury's geological history. In
81 a broader perspective, such a conclusion could also be applied to explain the absence of kilometer-
82 sized constructional volcanoes resulting from explosive eruptions. This is because the horizontally
83 compressive stresses prevailing in the crust of Mercury, due to global contraction, can hinder

84 magma ascent (*Byrne et al.*, 2014) and thus not allow explosive constructional volcanoes to form.
85 In this analysis, however, we propose a hypothesis in which the absence of small-volume explosive
86 volcanoes can be resolved through wide dispersal of the ballistic pyroclastic material around the
87 vent due to the specific conditions prevailing on Mercury's surface. Such dispersal would prevent
88 the formation of constructional edifices resolvable with MESSENGER imagery and topographical
89 data. Therefore, under this interpretation, small-volume explosive volcanoes could be present on
90 the surface of Mercury, but at present we do not have data suitable to detect them.

91 **2 The mechanism of the formation of pyroclastic cones**

92 Whether a volcanic eruption is effusive or explosive depends on the amount of volcanic
93 gases dissolved within the magma and/or the availability of the external volatiles that magma can
94 interact with during its ascent (*Cashman et al.*, 1999). Volcanic gases or external volatiles, in
95 sufficient volumes, are able to transport exploded rock fragments (“pyroclasts”) from the vent
96 according to their sizes either ballistically and/or by turbulent jets (e.g., *Wilson and Head*, 1994;
97 *Riedel et al.*, 2003). However, those transport mechanisms are heavily influenced by the presence
98 of an atmosphere. On airless bodies with an almost perfect vacuum, such as Mercury, the Moon,
99 or Jupiter’s moon Io, the transport mechanism is simpler as there are no interactions (or they are
100 so insignificant that they can be neglected) of the ejected particles with the atmosphere. Material
101 is therefore ejected from the vent along ballistic trajectories only, without particle deceleration by
102 atmospheric drag.

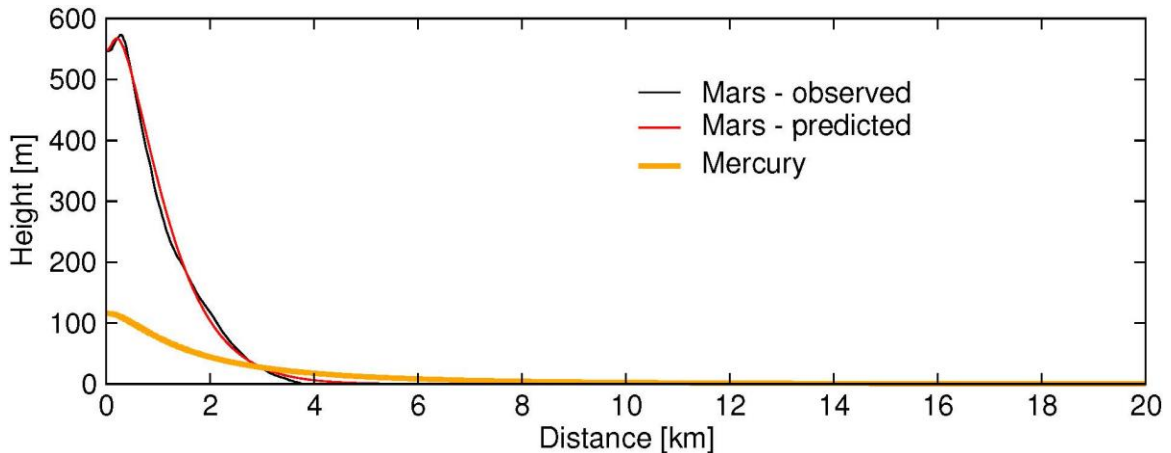
103 The final shape of explosive volcanoes on airless bodies is therefore controlled by the
104 ballistic ranges of particles, which depends mainly on ejection velocity and gravity, and by the
105 subsequent redistribution of the material by avalanches, which occur when the flank slope of the
106 cone exceeds the angle of repose (e.g., *Riedel et al.*, 2003). However, as shown in the example of
107 putative Martian scoria cones by *Brož et al.* (2014), it is difficult to achieve the angle of repose on
108 a body with a low-density or absent atmosphere and with substantially lower surface gravity than
109 on Earth. This is because particles are spread over a much larger area on such bodies, even if they
110 were thrown out by an explosion with an otherwise identical set of parameters as on a larger world
111 with an atmosphere. As a consequence, on Mars the erupted volumes of pyroclasts are not large
112 enough for the flank slopes to attain the angle of repose, in contrast with Earth where this is
113 common (and hence can be attained with lower erupted volumes). Martian analogues therefore
114 show gentler flank slopes and larger basal diameters (*Brož et al.*, 2015).

115 Although the current pressure on Martian surface is only about 600 Pa and the air density
116 is a factor of 100 lower than on Earth, the air drag on Mars can significantly affect the
117 transportation of ejected particles and hence the final shapes of pyroclastic features. Ballistic
118 pyroclastic particles would be spread even farther if Mars had no atmosphere at all. Therefore
119 features on airless bodies form with even gentler flank slopes, and hence more subtle topography,
120 than observed on Earth or even Mars (e.g., *Kereszturi & Németh*, 2013; *Brož et al.*, 2015). To
121 investigate these variations and to predict possible shapes of such small-scale explosive volcanoes
122 on Mercury we conducted numerical simulations, based on those by *Brož et al.* (2014) for Mars,
123 which calculate the ballistic trajectories of particles ejected under different conditions plausible
124 for Mercury, and trace the cumulative deposition from repeated ejections of particles over time
125 (for details about the used model see sections S1-S3 in the Supporting Information [*Brož et al.*,
126 2014; *Gouhier and Donnadieu*, 2010; *Harris et al.*, 2012]).

127 The ejection speed, which is independent of the particle size in our model, is described by
 128 a log-normal probability function with standard deviation σ_μ and mean $\log_{10}\mu$, where μ is the most
 129 probable ejection speed. The ejection angle, measured from the vertical, is characterized by a
 130 normal distribution centered at 0 with standard deviation σ_α which represents the mean angular
 131 radius of the ejection cone (see Figures S1-S4 in the Supporting Information for details). The shape
 132 of the ballistic feature is thus fully determined by only three parameters (μ , σ_μ , and σ_α) and by the
 133 gravitational acceleration at the surface of the planet (which is almost identical for Mercury and
 134 Mars, i.e., a mean gravity of 3.7 m/s^2 versus 3.71 m/s^2). For Mars, *Brož et al.* (2014, 2015)
 135 attempted to reproduce the shapes of the putative scoria cones using Earth-like values of σ_μ and
 136 including the effect of air resistance. They found that the largest known scoria cones on Mars are
 137 consistent with $\mu \approx 100 \text{ m/s}$ and $\sigma_\alpha \approx 30^\circ$. For Mercury, we assume that air resistance is negligible
 138 and the ballistic trajectory of a particle depends only on its initial speed and ejection angle.

139 3 The shapes of pyroclastic volcanoes on airless bodies

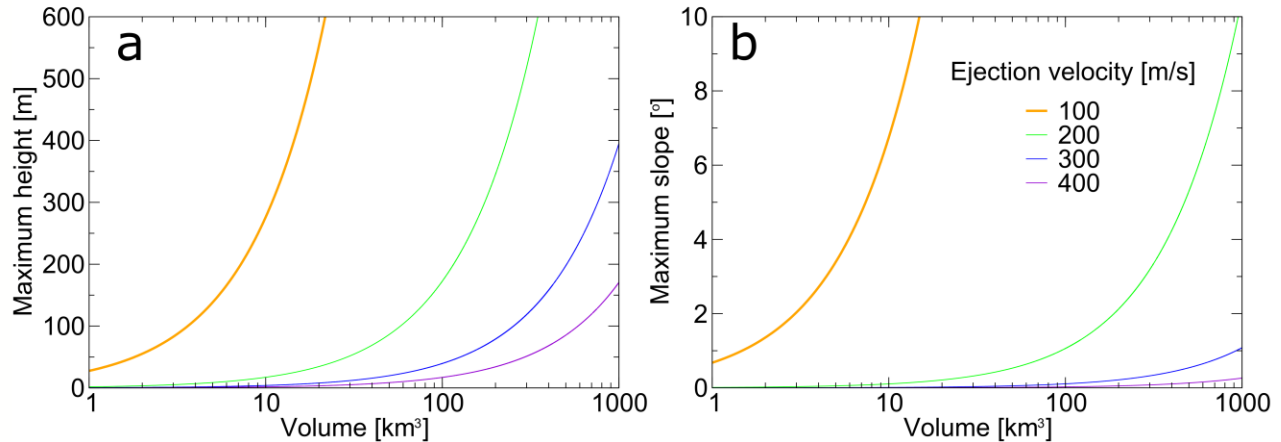
140 The lack of identified low-volume volcanoes on Mercury, and hence the unavailability of
 141 any data about their volumes, motivates us to assume in a first pass that pyroclastic cones would
 142 be formed by the same amount of material on Mercury as the most voluminous Martian putative
 143 scoria cone (4.2 km^3 : *Brož and Hauber, 2012; Brož et al., 2015*), and that the parameters of the
 144 eruption would be the same on both bodies (see description of Figure 1 for details, or *Brož et al.,*
 145 *2014; 2015*). The only difference in model setup we consider here is the lack of an atmosphere for
 146 Mercury.



147
 148 Figure 1: Comparison of the observed topographic profile of one putative 4.2 km^3
 149 Martian scoria cone (in black, the cone informally named UC2 in *Brož et al., 2015*) with the
 150 profiles of similar volumes computed for speed $\mu=100 \text{ m/s}$, log-normal distribution scaling
 151 $\sigma_\mu=0.2$ and radius of ejection cone $\sigma_\alpha= 30^\circ$ in the environment of Mars (in red) and Mercury (in
 152 orange). The absence of an atmosphere on Mercury causes ~ 4.4 times wider dispersion of
 153 particles and the formation of feature only $\sim 18\%$ as high compared with Mars.

154 The results of our modeling show (Figure 1) that, although $\sim 99\%$ of the ejected material
 155 on Mars would be deposited within a circle $\sim 4.5 \text{ km}$ in radius, the same amount of material on
 156 Mercury would be deposited within an area $\sim 20 \text{ km}$ in radius, i.e., about 4.4 times farther. As a
 157 consequence, the material is dispersed on Mercury over an area ~ 20 times larger than on Mars.
 158 For the same volume of ejected material (4.2 km^3) on Mercury as on Mars, the wider dispersal

159 would cause a dramatic decrease in the height of the cone and a corresponding reduction in slope
 160 angles (for definition of the slope angle, see section S4 in the Supporting Information). On Mars,
 161 the deposition of material would cause the formation of conical edifices with a height of ~570
 162 meters, and flanks would retain a slope angle of 24° in the steepest part of the profile (red profile
 163 in Fig. 1). In contrast, the eruption of the same volume of material on Mercury would create a
 164 surface feature ~100 meters high and with flank slopes which would maximally reach only 2.8°
 165 (orange profile in Fig. 1). The reduction in height of the resulting feature would be so substantial,
 166 that the shape would not be an obvious cone at all, but rather a slightly elevated broad and gently
 167 sloping hump with subtle topography.



168
 169 Figure 2: Dependency of the maximum height (panel a) and maximum flank slopes
 170 (panel b) of a pyroclastic edifice on the total volume of erupted material in the environment of
 171 Mercury. Lines of different colors show results for different ejection speeds, namely for 100 m/s
 172 (orange), 200 m/s (green), 300 m/s (blue), and 400 m/s (violet). Parameters σ_α and σ_μ are as
 173 described in the caption of Figure 1.

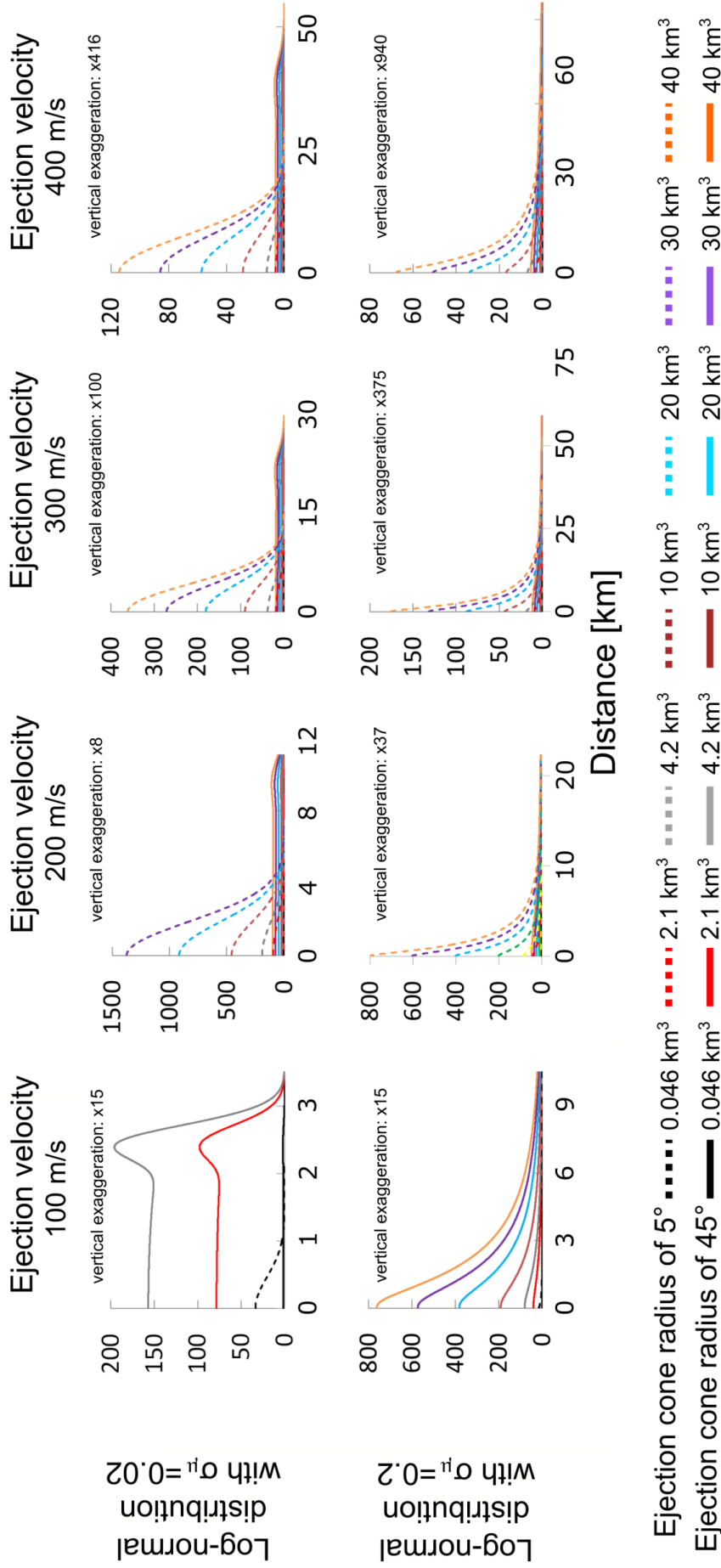
174 In the next step, we investigate how the maximum height and flank slopes of ballistically
 175 emplaced features would be affected by the variation of the volume of ejected material in the
 176 Mercurian environment. The results are summarized in Figure 2. To achieve the same height of
 177 our test-case cone on Mars (~570 m), the volume of erupted material on Mercury must be increased
 178 by factor of ~5 (corresponding to ~20.7 km³ of ejected material) for the same initial speeds and
 179 ejection angles we considered earlier. If the material is ejected at higher initial speeds on Mercury
 180 than expected for Mars, the amount of material necessary to construct a landform of such height
 181 must further increase (Figure 2a). However, the results also show that even if the height of the
 182 Martian cone could be reached on Mercury, the resulting shape would be different. The final
 183 edifices would have gentler flank slopes (maximally 13.8° on Mercury versus 24° on Mars in the
 184 steepest part of the cones) for the same sets of parameters for both eruptions, including an ejection
 185 speed of 100 m/s. However, if the initial speeds of ejected particles were higher on Mercury than
 186 on Mars, the flank slopes of the final edifices would be even more topographically subtle;
 187 specifically, for ejection speed of 200 m/s, 300 m/s and 400 m/s the final slope angles would be
 188 maximally reaching the value of 3.5° , 1.6° , and 0.9° respectively.

189 Until now, we have considered only solutions based on the assumption that explosive
 190 volcanism would occur on Mercury with a similar set of parameters as determined for low-volume
 191 explosive eruptions on Mars (Brož *et al.*, 2014; 2015 and references therein). However, such

192 assumptions may not be equally applicable to airless bodies. Due to the lack of an atmosphere,
193 some (or all) of these parameters may differ drastically from those Martian values.

194 For example, *Wilson and Head* (2003) suggested that the lack of atmosphere on the Moon
195 would affect the way in which the ascending picritic magma would be degassed once it reached
196 the lunar surface. Once the tip of a dike breaks through the crust, free gas at the tip would escape
197 quickly so the lava foam forming the upper part of the dike would be exposed to the vacuum. The
198 gas bubbles formerly at a pressure of ~ 100 MPa within the lava foam would therefore rapidly
199 expand. As a consequence, an expansion wave(s) able to travel at high speed downward through
200 the dike would be generated. This wave would likely cause rapid disintegration of the lava foam
201 and hence rapid release of the trapped volcanic gases, leading to much higher ejection speeds for
202 the small pyroclastic particles (up to 760 m/s) than speeds common on Earth and Mars. Also, *Glaze*
203 *and Baloga* (2000) and *Wilson and Head* (2007) assumed that the presence of an atmosphere and
204 its associated density can also affect the ejection angles at which magma fragments are ejected,
205 such that on bodies with lower atmospheric pressure, wider ($\sigma_\alpha \geq 30^\circ$) ejection cones than on Earth
206 should be expected.

207 Since the angular radius of an ejection cone (σ_α) and the values of ejection speeds (μ , σ_μ)
208 are unknown for Mercury, we performed a set of numerical runs with parameters that spanned a
209 range of plausible values. Specifically we investigated how narrow ($\sigma_\alpha = 5^\circ$) and wide ($\sigma_\alpha = 45^\circ$)
210 ejection cones, the initial speed of ejected particles ($\mu = 100$ m/s, 200 m/s, 300 m/s, and 400 m/s),
211 and scale in the coefficient of the log-normal distribution of ejection speed (σ_μ 0.02 and 0.2) would
212 change the distribution of the ejected particles and thus the resulting shapes of explosively
213 emplaced, constructional volcanic features on Mercury. The results are summarized in Figure 3,
214 where the eight panels show the topography generated for a given set of the parameter values
215 discussed above. The dashed and solid lines in the panels show predicted topographies for narrow
216 and wide ejection angles respectively, and different colors show variations in volume. Only those
217 solutions that do predict slopes at the angle of repose (30°) are shown here as the model cannot
218 simulate additional transport by subsequent avalanching and hence the additional growth in
219 diameter and height.



221 Figure 3: Comparison of the predicted topographies of putative explosive volcanic
222 features on Mercury, as a function of ejection speeds (increasing from left to right), scaling
223 parameter σ_μ of the log-normal distribution of ejection speed (increasing from up to down),
224 volumes (marked by different colors), and the angular radius of ejection cone (dashed versus
225 solid lines). Note the vertical exaggeration, which varies between panels. For $\sigma_\alpha = 45^\circ$, only
226 ejection angles smaller than 60° are considered.

227 The results show that the larger the angular radius of the ejection cone is or the higher the
228 ejection speed, or the larger the coefficient of log-normal distribution, or a combination thereof,
229 the greater the area over which the ejecta is dispersed. For a fixed eruption volume, wider dispersal
230 necessarily leads to a decrease in the height of the final shape and to proportionately shallower
231 flank slopes. This finding is in agreement with previous predictions of the explosive eruptions on
232 the Moon or Mars (*Wilson and Head, 2003; Brož et al., 2015*) and also with the observations of
233 large *faculae* (up to 260 km in diameter) surrounding putative volcanic vents on Mercury, which
234 show little ($<1^\circ$) or no topographic relief at all (*Thomas et al., 2014a*).

235 We also focus on the effect of the ejected volume on the shapes of modeled features;
236 however, the absence of observational evidence of kilometer-sized explosive volcanoes on
237 Mercury required us again to assume a range of possible erupted volumes. We chose volumes from
238 0.046 km^3 up to 40 km^3 with intermediate steps of 2.1 km^3 , 4.2 km^3 , 10 km^3 , 20 km^3 , and 30 km^3 .
239 The lower limit was chosen to resemble the typical volume of terrestrial scoria cones (determined
240 from 986 edifices based on data from *Pike [1978]* and *Hasenaka and Carmichael [1985]*) and the
241 upper limit of 40 km^3 was chosen as this is the median volume of putative large-scale explosive
242 vents on the surface of Mercury (*Thomas et al., 2014a*). We chose the median volume of large
243 vents as the upper limit of our experiments because if the explosive eruptions that excavated these
244 large vents ejected only crustal material, and under the assumption that no subsurface withdrawal
245 of material occurred, then the volume of their pyroclastic deposits would be approximately equal
246 to the volume of their source vents. However, it is currently unknown what the typical volume
247 ratio of juvenile volcanics to crustal material is in *faculae* on Mercury (*Thomas et al., 2015a*),
248 therefore we consider the volume of the large vents to be a lower limit for the volumes of their
249 pyroclastic deposits. Thus, we can make only a first approximation of the topography generated
250 by the large-scale vent-forming eruptions.

251 Our modeling reveals that for particles ejected at high initial speeds and with a large
252 angular radius of the ejection cone, a wide and flat edifice with low topography and very gentle
253 flank slopes forms regardless of the chosen erupted volume. This landform shape is a result of the
254 dispersal of the erupted material across such a large area that even an amount of material larger by
255 three orders of magnitude than is typical for Earth would be insufficient to build a substantial (at
256 least several hundreds of meters high) topographic feature composed of accumulated pyroclastic
257 ejecta. In other words, conical edifices would not be formed. Similar shapes would be achieved
258 even with narrow ejection angles if the particles were ejected at speeds near the upper range of our
259 considered values. Such low-relief shapes are in contrast to pyroclastic volcanoes on Earth or
260 Mars, where a conical edifice is generated, because atmospheric drag decreases the speed of the
261 ejected particles and prevents widespread dispersal of the particles from the vent (e.g., *Riedel et*
262 *al., 2003; Brož et al., 2014*).

263 To produce a kilometers-wide and hundreds-of-meters-high constructional edifice with a
264 conical shape on Mercury, it is necessary for the initial speeds to be within the low range of
265 considered values, and/or for the material to be ejected within an exceptionally small range of

266 ejection angles (less than 5°). However, the lack of identified conical features on Mercury
267 plausibly of volcanic origin (see *Fassett et al.*, 2009), of which >90% of its surface is now covered
268 by high-resolution images of suitable illumination (>90% of the MESSENGER ~166 m/pixel
269 global mosaic is composed of images with solar incidence angles >68°, which enable visual
270 observations of hundred meter-scale topographic features) enabling their detection, suggests that,
271 although theoretically possible, these parameters are improbable. Moreover the environmental
272 properties do not favor such conditions at all: the absence of an atmosphere tends to increase the
273 initial speeds of ejected particles due to the rapid expansion of volcanic gasses several times than
274 is typical on Earth or Mars (e.g., *Wilson and Head*, 2003; *Brož et al.*, 2014; 2015; *Thomas et al.*,
275 2015b), and also cause a greater spread of ejection angles around a mean ejection angle (*Glaze
276 and Baloga*, 2000). These controlling effects of an atmosphere, or for Mercury the lack thereof,
277 directly promote conditions inimical to the formation of kilometer-sized conical edifices on this
278 body.

279 We therefore assume that wide ejection cones and high ejection speeds are characteristic
280 aspects of explosive volcanism on Mercury, not only for those vents associated with dozens of ten-
281 kilometer-scale bright putative pyroclastic units (faculae) and formed by large volume eruptions
282 (*Thomas et al.*, 2015a, 2015b; *Jozwiak et al.*, 2018), where the width and sometimes compound
283 nature of the vent suggests broad dispersal (e.g., *Rothery et al.*, 2014), but also for those that would
284 potentially result from the emplacement of low volumes of pyroclastic material. If so, the low
285 volume of ballistically emplaced pyroclastic volcanoes on Mercury would not form pronounced
286 conical edifices as common on Earth and Mars, but instead would result in very topographically
287 subtle features difficult or even impossible to detect with current data. For example, if we assume
288 that the same amount of material as is commonly erupted in a single event on Earth (0.046 km³)
289 or on Mars (4.2 km³) is dispersed from a vent with an initial speed of 300 m/s comparable to the
290 average speed calculated from the dispersal of particles forming faculae surrounding putative
291 Mercurian volcanic vents of 284 m/s (*Thomas et al.*, 2015a, 2015b) then the maximum final
292 thickness of an accumulated pyroclastic pile would be less than 0.02 m and 1.25 m respectively.
293 Such a topographically insignificant landform would likely quickly be destroyed or significantly
294 modified by impact gardening or other surface modifications processes (including subsequent
295 volcanism). This would make the discovery of such volcanoes a complicated task even with the
296 high-resolution data expected to be returned by the ESA–JAXA BepiColombo spacecraft mission
297 (*Benkhoff et al.*, 2010; *Rothery et al.*, 2010).

298 Another aspect which has to be considered in the attempt to find these pyroclastic features
299 is their survivability on the surface of Mercury. Their subtle topography and the resulting easy
300 erodibility may cause that all such features could be already destroyed by resurfacing events.
301 However, the example of the Moon, which has had a similar history of impact erosion to Mercury
302 (*Fassett and Minton*, 2013) and on which evidences of pyroclastic deposits has been observed both
303 from orbit and by *in situ* investigation, indicates that if small-scale volcanic constructions are
304 widespread enough, evidence of their presence can survive billions of years of geological time and
305 therefore should also leave some detectable traces on the surface of Mercury.

306 **4 Conclusions**

307 Our study shows that the environmental properties on Mercury lead to wide dispersal of
308 pyroclastic ejecta and preclude the formation of constructional volcanic edifices of the forms
309 recognized on Earth and Mars. The final constructional shapes on Mercury may instead resemble

310 a wide and very gentle blanket of pyroclastic deposits. However, the real width of the Mercurian
311 pyroclastic deposits could be even greater than generally considered (e.g., Kerber *et al.*, 2011;
312 Thomas *et al.* 2014a,b). This is because the areal extent of the spectral anomalies, which commonly
313 denote large deposits interpreted as pyroclasts (e.g., Thomas *et al.*, 2015b), or morphological
314 properties (e.g. breaks in slope angles) of explosive volcanic edifices (e.g. Brož *et al.*, 2015), are
315 measured by approaches that conservatively exclude the tenuous outer fringes of deposits which
316 are barely detectable with current data (Besse *et al.*, 2015, 2018). This approach, however, likely
317 underestimates the volume of erupted pyroclastic material and in turn supports average values of
318 initial speeds of ejected particles that are too low. Therefore, in reality, the pyroclastic deposits
319 emplaced as the result of low-volume eruptions on Mercury (and also on the Moon) may be even
320 thinner, in the range of centimeters to millimeters, so the volume necessary to create a detectable
321 landform with orbital data might not be reached at all. For this reason, finding evidence of such
322 explosive volcanic activity, such as the spherules of volcanic glasses similar to those discovered
323 on the Moon, may require currently impractical *in situ* investigation. It may be more helpful, then,
324 for future investigation of low volume pyroclastic deposits on Mercury (e.g., with data returned
325 by the BepiColombo mission) to focus on physical and chemical variations of the surface material,
326 rather than to search for subtle topographic signatures of those pyroclastic deposits formed by
327 explosive volcanism.

328 Because there are other terrestrial bodies within the Solar System without an atmosphere
329 (e.g., the Moon or Io), our results have implications beyond Mercury. We predict that on those
330 airless bodies steep conical edifices cannot be constructed purely by the ballistic emplacement and
331 accumulation of cold pyroclastic particles. Other processes, such as periodic effusive eruptions
332 causing spattering of the ejected particles and/or formation of lava flows, may be required to
333 steepen edifices into cones, such as those observed in the Marius Hills region on the Moon
334 (Lawrence *et al.* 2013). Per nomenclature for Earth, cones constructed in this fashion are more
335 properly referred to as “composite cones” and as a consequence, the concept of pyroclastic cones
336 or scoria cones on airless bodies may not apply.

337 **References**

- 338 Benkhoff, J., Van Casteren, J., Hayakawa, H., Fujimoto, M., Laakso, H., Novara, M., ... & Ziethe,
339 R. (2010), BepiColombo—Comprehensive exploration of Mercury: Mission overview and
340 science goals. *Planetary and Space Science*, 58(1-2), 2-20, doi:10.1016/j.pss.2009.09.020.
- 341 Besse, S., Doressoundiram, A., & Benkhoff, J. (2015). Spectroscopic properties of explosive
342 volcanism within the Caloris basin with MESSENGER observations. *Journal of*
343 *Geophysical Research: Planets*, 120(12), 2102-2117, doi:10.1002/2015JE004819.
- 344 Besse, S., Dorressoundiram, A., & Griton, L. (2018), Analysis of Pyroclastic Deposits Using
345 MESSENGER MASCS Observations. In *Mercury: Current and Future Science of the*
346 *Innermost Planet* (Vol. 2047).
- 347 Brož, P. & Hauber, E. (2012), A unique volcanic field in Tharsis, Mars: pyroclastic cones as
348 evidence for explosive eruptions. *Icarus* 218, 88–99, doi:10.1016/j.icarus.2011.11.030.
- 349 Brož, P., Čadek, O., Hauber, E., & Rossi, A.P. (2014), Shape of scoria cones on Mars: Insights
350 from numerical modeling of ballistic pathways. *Earth and Planetary Science Letters* 406,
351 14–23, doi:10.1016/j.epsl.2014.09.002.
- 352 Brož, P., Čadek, O., Hauber, E., & Rossi, A.P. (2015), Scoria cones on Mars: detailed investigation
353 of morphometry based on high-resolution digital elevation models. *Journal of Geophysical*
354 *Research: Planets* 120, 1512–1527, doi:10.1002/2015JE004873.

355 Brož, P., Hauber, E., Wray, J. J., & Michael, G. (2017), Amazonian volcanism inside Valles
356 Marineris on Mars. *Earth and Planetary Science Letters* 473, 122–130,
357 doi:10.1016/j.epsl.2017.06.003.

358 Byrne, P.K., Klimczak, C., Sengör, A.M.C., Solomon, S.C., Watters, T.R., & Hauck, S.A. (2014),
359 Mercury's global contraction much greater than earlier estimates. *Nature Geoscience* 7, 301–
360 307, doi:10.1038/NGEO2097.

361 Byrne, P. K., Ostrach, L. R., Fassett, C. I., Chapman, C. R., Denevi, B. W., Evans, A. J., ... &
362 Solomon, S. C. (2016), Widespread effusive volcanism on Mercury likely ended by about
363 3.5 Ga. *Geophysical Research Letters* 43 (14), 7408-7416, doi:10.1002/2016GL069412.

364 Cashman, K. V., Sturtevant, B., Papale, P., & Navon, O. (1999), Magmatic Fragmentation. In
365 *Encyclopedia of volcanoes*. Edited by H. Sigurdsson, pp. 421–430, Academic Press, San
366 Diego, California.

367 Denevi, B. W., Ernst, C. M., Meyer, H. M., Robinson, M. S., Murchie, S. L., Whitten, J. L., & et
368 al. (2013), The distribution and origin of smooth plains on Mercury. *Journal of Geophysical*
369 *Research: Planets* 118, 891–907, doi:10.1002/jgre.20075.

370 Fassett, C.I. et al., (2009), Caloris impact basin: Exterior geomorphology, stratigraphy,
371 morphometry, radial sculpture, and smooth plains deposits. *Earth and Planetary Science*
372 *Letters* 285 (3–4), 297–308, doi:10.1016/j.epsl.2009.05.022.

373 Fassett, C. I., & Minton, D. A. (2013), Impact bombardment of the terrestrial planets and the early
374 history of the Solar System. *Nature Geoscience*, 6(7), 520–524, doi:10.1038/geo1841.

375 Glaze, L.S., & Baloga, S.M. (2000), Stochastic–ballistic eruption plumes on Io. *Journal of*
376 *Geophysical Research: Planets* 105, 17579–17588, doi:10.1029/1999JE001235.

377 Gouhier, M., and F. Donnadieu (2010), The geometry of Strombolian explosions: insights from
378 Doppler radar measurements, *Geophysical Journal International* 183, 1376–1391,
379 doi:10.1111/j.1365-246X.2010.04829.x.

380 Harris, A. J. L., M. Ripepe, and E. A. Hughes (2012), Detailed analysis of particle launch
381 velocities, size distributions and gas densities during normal explosions at Stromboli, *Journal*
382 *of Volcanology and Geothermal Research* 231–232, 109–131,
383 doi:10.1016/j.jvolgeores.2012.02.012.

384 Hasenaka, T., & Carmichael, I. S. E. (1985), The cinder cones of Michoacán–Guanajuato, central
385 Mexico: Their age, volume and distribution, and magma discharge rate. *Journal of*
386 *Volcanology and Geothermal Research* 25, 104–124, doi:10.1016/0377-0273(85)90007-1.

387 Hauber, E., Bleacher, J., Gwinner, K., Williams, D. A., & Greeley, R. (2009), The topography and
388 morphology of low shields and associated landforms of plains volcanism in the Tharsis
389 region of Mars. *Journal of Volcanology and Geothermal Research* 185(1–2), 69–95,
390 doi:10.1016/j.jvolgeores.2009.04.015.

391 Head, J. W., Murchie, S. L., Prockter, L. M., Robinson, M. S., Solomon, S. C., Strom, R. G., & et
392 al. (2008), Volcanism on Mercury: Evidence from the first MESSENGER flyby. *Science*
393 321(5885), 69–72, doi:10.1126/science.1159256.

394 Head, J. W., Murchie, S. L., Prockter, L. M., Solomon, S. C., Chapman, C. R., Strom, R. G., ... &
395 Dickson, J. L. (2009), Volcanism on Mercury: Evidence from the first MESSENGER flyby
396 for extrusive and explosive activity and the volcanic origin of plains. *Earth and Planetary*
397 *Science Letters*, 285(3-4), 227-242, doi:10.1016/j.epsl.2009.03.007. Head, J. W., Chapman,
398 C. R., Strom, R. G., Fassett, C. I., Denevi, B. W., Blewett, D. T., & et al. (2011), Flood
399 volcanism in the northern high latitudes of Mercury revealed by MESSENGER. *Science*
400 333(6051), 1853–1856, doi:10.1126/science.1211997.

401 Jozwiak, L. M., Head, J. W., & Wilson, L. (2018), Explosive volcanism on Mercury: Analysis of
402 vent and deposit morphology and modes of eruption. *Icarus* 302, 191-212, doi:
403 10.1016/j.icarus.2017.11.011.

404 Kerber, L., Head, J.W., Solomon, S.C., Murchie, S.L., Blewett, D.T., & Wilson, L. (2009),
405 Explosive volcanic eruptions on Mercury: eruption conditions, magma volatile content, and
406 implications for interior volatile abundances. *Earth and Planetary Science Letters* 285 (3–
407 4), 263–271, doi:10.1016/j.epsl.2009.04.037.

408 Kerber, L., J. W. Head, D. T. Blewett, S. C. Solomon, L. Wilson, S. L. Murchie, M. S. Robinson,
409 B. W. Denevi, and D. L. Domingue (2011), The global distribution of pyroclastic deposits
410 on Mercury: The view from MESSENGER flybys 1–3. *Planet. Space Sci.*, 59, 1895–1909,
411 doi:10.1016/j.pss.2011.03.020

412 Kereszturi, G., & Németh, K. (2013), Monogenetic basaltic volcanoes: genetic classification,
413 growth, geomorphology and degradation. In: Németh, K. (Ed.), *Updates in Volcanology –*
414 *New Advances in Understanding Volcanic Systems*. InTech.

415 Klimczak, C., Crane, K. T., Habermann, M. A., & Byrne, P. K. (2018), The spatial distribution of
416 Mercury's pyroclastic activity and the relation to lithospheric weaknesses. *Icarus* 315, 115–
417 123, doi: 10.1016/j.icarus.2018.06.020.

418 Lawrence, S.J., et al. (2013), LRO observations of morphology and surface roughness of volcanic
419 cones and lobate lava flows in the Marius Hills. *Journal of Geophysical Research: Planets*
420 118, doi:10.1002/jgre.20060.

421 Pike, R. J. (1978), Volcanoes on the inner planets: Some preliminary comparisons of gross
422 topography. *Proc. Lunar Sci. Conf. IX*, Abstract 3239–3273.

423 Riedel, C., Ernst, G.G.J., & Riley, M. (2003), Controls on the growth and geometry of pyroclastic
424 constructs. *Journal of Volcanology and Geothermal Research* 127, 121–152,
425 doi:10.1016/S0377-0273(03)00196-3.

426 Rothery, D. A., Marinangeli, L., Anand, M., Carpenter, J., Christensen, U., Crawford, I. A. & et
427 al. (2010), Mercury's surface and composition to be studied by BepiColombo. *Planetary and*
428 *Space Science* 58(1-2), 21–39. doi:10.1016/j.pss.2008.09.001.

429 Rothery, D. A., Thomas, R. J., & Kerber, L. (2014), Prolonged eruptive history of a compound
430 volcano on Mercury: Volcanic and tectonic implications. *Earth and Planetary Science*
431 *Letters* 385, 59-67, doi: 10.1016/j.epsl.2013.10.023.

432 Thomas, R. J., Rothery, D. A., Conway, S. J., & Anand, M. (2014a), Mechanisms of explosive
433 volcanism on Mercury: Implications from its global distribution and morphology. *Journal*
434 *of Geophysical Research: Planets* 119, 2239–2254, doi:10.1002/2014JE004692.

435 Thomas, R. J., Rothery, D. A., Conway, S. J., & Anand, M. (2014b), Long-lived explosive
436 volcanism on Mercury. *Geophysical Research Letters* 41, 6084–6092,
437 doi:10.1002/2014GL061224.

438 Thomas, R.J., Lucchetti, A., Cremonese, G., Rothery, D.A., Massironi, M., Re, C., Conway, S.J.,
439 & Anand, M. (2015a), A cone on Mercury: analysis of a residual central peak encircled by
440 an explosive volcanic vent. *Planetary and Space Science* 108, 108–116, doi:
441 10.1016/j.pss.2015.01.005.

442 Thomas, R. J., Rothery, D. A., Conway, S. J., & Anand, M., (2015b), Explosive volcanism in
443 complex impact craters on Mercury and the Moon: Influence of tectonic regime on depth of
444 magmatic intrusion. *Earth and Planetary Science Letters* 431, 164–172,
445 doi:10.1016/j.epsl.2015.09.029.

446 Wilson, L., & Head, J.W. (1994), Review and analysis of volcanic eruption theory and re-
447 lationships to observed landforms. *Reviews of Geophysics* 32, 221–263,
448 doi:10.1029/94RG01113.

449 Wilson, L., & Head, J. W. (2003), Deep generation of magmatic gas on the Moon and implications
450 for pyroclastic eruptions. *Geophysical Research Letters* 30(12), 1605,
451 doi:10.1029/2002GL016082.

452 Wilson, L., & Head, J.W. (2007), Explosive volcanic eruptions on Mars: tephra and ac-cretionary
453 lapilli formation, dispersal and recognition in the geological record. *Journal of Volcanology
454 and Geothermal Research* 163, 83–97, doi:10.1016/j.jvolgeores.2007.03.007.

455 Wright, J., Rothery, D. A., Balme, M. R., & Conway, S. J. (2018), Constructional volcanic edifices
456 on Mercury: Candidates and hypotheses of formation. *Journal of Geophysical Research:
457 Planets* 123, doi:10.1002/2017JE005450.

458

459 **Acknowledgments**

460

461 We thank the responsible Editor, Andrew J. Dombard, and two reviewers, Paul Byrne and
462 Sebastien Besse, for constructive comments and inspiring suggestions. The results of numerical
463 simulations used in the paper can be found at <http://doi.org/10.5281/zenodo.1442406>.